

Optics Letters

High power picosecond green and deep ultraviolet generations with an all-fiberized MOPA

LEI PAN,*  JIHONG GENG, AND SHIBIN JIANG

Advalue Photonics Inc., 2700 E. Bilby Rd., Tucson, Arizona 85706, USA

*Corresponding author: lpan@advaluephotonics.com

Received 8 August 2022; revised 25 August 2022; accepted 7 September 2022; posted 12 September 2022; published 27 September 2022

We demonstrate high power picosecond green and deep ultraviolet (DUV) lasers based on an all-fiberized master oscillator power amplifier (MOPA). The main power amplifier is fabricated with a highly Yb-doped large mode area (LMA) silicate glass fiber. It delivers 75.2-W laser output at 1029 nm with a pulse repetition rate of 10 MHz and a pulse duration of 70 ps. With a lithium triborate (LBO) crystal, a 43.0-W green output at 514.5 nm has been achieved with a pulse duration of 55 ps. With a caesium lithium borate (CLBO) crystal, a 14.5-W picosecond DUV output at 257 nm has been generated, which is the highest power for the all-fiber based DUV laser, to the best of our knowledge. © 2022 Optica Publishing Group

<https://doi.org/10.1364/OL.472644>

Compared with infrared (IR) and visible lasers, the deep ultraviolet (DUV) radiation has much higher photon energy, smaller achievable focal spot, and larger absorption cross section for most materials. The high power and short pulse DUV lasers are of great interest for many scientific, industrial, and medical applications, like breakdown spectroscopy [1], precise micromachining [2], semiconductor photolithography [3], and single-molecule imaging [4]. In a free electron laser, a pulsed DUV laser is used to illuminate the semiconductor cathode to create an electron beam for a linear accelerator. For example, for the newly developed Linac Coherent Light Source II (LCLS-II), it will be operating at a high repetition rate of up to 1 MHz; therefore, a powerful and high repetition rate DUV laser is required to work as an injector drive laser [5].

The DUV laser is traditionally generated by nonlinear frequency conversion of an IR solid-state or fiber laser. Compared with bulk solid-state lasers, fiber lasers have the advantages of compactness, robustness, high reliability, and being maintenance free. However, due to the tight confinement and the long geometry, the fiber laser pulse energy and peak power are significantly limited by nonlinear effects such as self-phase modulation (SPM) and stimulated Brillouin scattering (SBS). Recently, there have been considerable efforts to address the challenges and achieve fiber-based DUV sources [6–10]. However, the highest DUV output power is 5.8 W with a sub-nanosecond pulse width [10].

In this work, we demonstrated high power picosecond green and DUV lasers based on an all-fiberized master oscillator power

amplifier (MOPA). The main power amplifier is fabricated with Advalue Photonics' recently developed highly Yb-doped large mode area (LMA) polarization-maintaining (PM) silicate glass fiber under patented technologies [11,12]. With a lithium triborate (LBO) crystal, a 43.0-W picosecond green output has been achieved with a 75.2-W IR output at 1029 nm. The green laser pulse width is ~55 ps with a repetition rate of 10 MHz. With a caesium lithium borate (CLBO) crystal, up to 14.5-W DUV at 257 nm has been generated, which is the highest power for an all-fiber-based DUV laser, to the best of our knowledge.

The schematic diagram of the laser system is shown in Fig. 1. The seed laser is a fast modulated distributed feedback (DFB) laser which generates ~70-ps full width at half maximum (FWHM) pulses with a repetition rate of 40 MHz and a 3-dB linewidth of 0.1 nm at 1029 nm. Since its output power is very low (tens of μ W), multi-stage Yb pre-amplifiers have been employed to increase the power to the tens of mW level. To set a pulse repetition rate, an acoustic optic modulator (AOM) works as a pulse picker. After the AOM, the pulse repetition rate is reduced to 10 MHz. A bandpass filter (BPF) centering at 1030 nm is used to remove the amplified spontaneous emission (ASE) at other wavelengths. Then the seed laser power is further increased by a booster Yb fiber amplifier. The booster amplifier is built with an LMA Yb-doped fiber 10/125PM. Its output power is intentionally limited to ~300 mW, which corresponds to a pulse energy of 30 nJ and a peak power of ~430 W. Further increasing the output power is possible, but the SFM effects will be significant. The SFM effects cause spectral broadening and may decrease the conversion efficiency in the second harmonic generation (SHG). The output from the booster fiber amplifier goes through a fiber isolator and is coupled to the main fiber amplifier by a $(2 + 1) \times 1$ pump combiner. The main amplifier is fabricated with the company proprietary silicate glass fiber. It is a step index fiber with a core numerical aperture (NA) lower than 0.04. It has a mode field diameter (MFD) of ~40 μ m with a length of only ~20 cm. Therefore, it can support hundred-kW peak power laser pulses without showing significant SBS and SRS issues. The glass fiber is a highly Yb-doped gain medium and the measured residual 976-nm pump laser is ~10% of the total. A fiberized mode adaptor is fabricated at the input end of the gain fiber to ensure highly efficient fundamental mode coupling from the pump combiner. An angle polished endcap is spliced at the output end to provide protection and eliminate any backreflection. The depicted high-power and high-efficiency

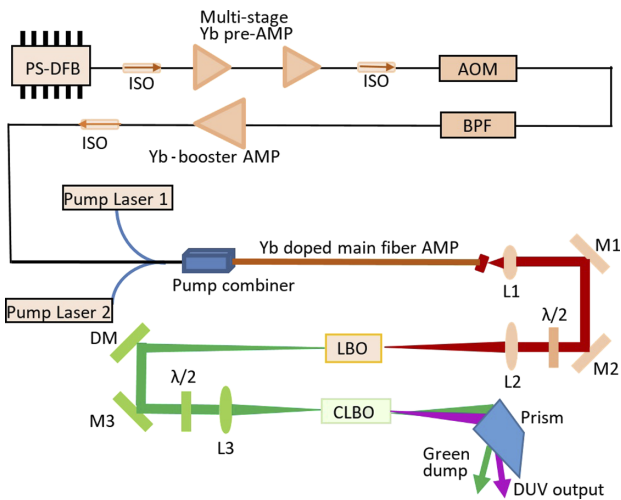


Fig. 1. Schematic diagram of the laser system. PS-DFB, picosecond distributed feedback laser; ISO, fiber isolator; AMP, amplifier; AOM, fiber coupled acoustic optic modulator; BPF, fiber bandpass filter; L, collimation/focusing lens; M, high reflection mirror; $\lambda/2$, half-wave plate; DM, dichroic mirror.

Yb-doped MOPA system is all PM fiber spliced without any free space optics. It generates a high power, alignment free, and linearly polarized IR output which is ready for SHG.

The main fiber amplifier output power versus pump power is shown in Fig. 2. The 1029-nm output power increases linearly with the 976-nm pump. At a pump power of 126 W, a 75.2-W output power has been achieved, corresponding to a slope efficiency of 64.6%. Considering the 300-mW input seed laser power, the net gain of the main fiber amplifier is ~24 dB. The Yb main fiber amplifier output is linearly polarized with a measured polarization extinction ratio (PER) of ~15 dB. The output beam quality is characterized by a Spiricon M2-200 M^2 meter which is shown in Fig. 3. The beam is a single-mode output with excellent M^2 values of 1.028 and 1.086 in the x and y direction, respectively. The inset picture in Fig. 3 shows the beam profile at the waist position of the beam caustic. The output pulse shape and pulse train measured by a fast photodiode (15 GHz) and an oscilloscope (12.5 GHz) are shown in Fig. 4. The pulse width is ~70 ps with a pulse repetition rate of 10 MHz, corresponding to a pulse energy of 7.5 μ J and a peak power of 107 kW.

As shown in Fig. 1, the high-power output from the all-fiberized MOPA is collimated (L1) and then focused (L2) to an LBO crystal for SHG. A half-wave plate with anti-reflection (AR) coating at 1029 nm is inserted before L2 for adjusting the IR polarization to a maximum SHG efficiency. The LBO crystal has a size of 3 mm \times 3 mm \times 35 mm with a type-I non-critical phase matching. It is held by an oven with a temperature setting of ~191°C. The SHG green (514.5 nm) laser output and conversion efficiency at different power levels are shown in Fig. 2. At a maximum IR (1029 nm) power of 75.2 W, 43.0 W of 514.5-nm picosecond green output has been achieved, corresponding to a conversion efficiency of 57.2%. As can be seen in the fitted curve, the SHG conversion efficiency increases with IR power; reaches a maximum at ~42-W IR power (@76.0 W of 976-nm pump), then slightly drops with the increase of the pump power. We believe this SHG conversion efficiency drop is related to nonlinear spectral broadening effects under a high peak power. Figure 5 shows the main fiber amplifier IR output spectrum

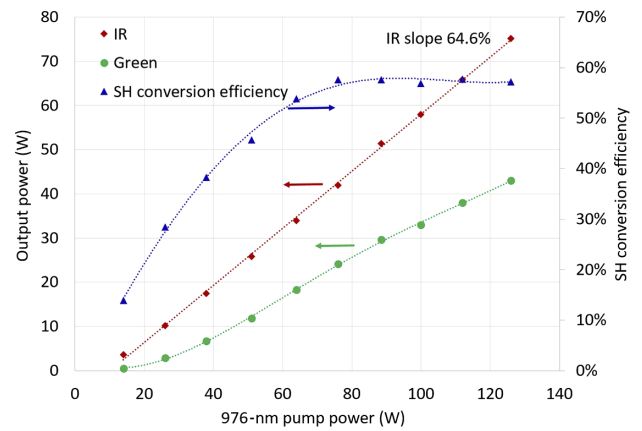


Fig. 2. Output powers of 1029-nm IR, 514.5-nm green, and harmonic conversion efficiency versus 976-nm pump power.

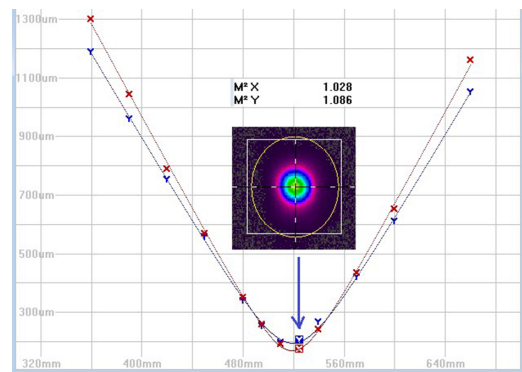


Fig. 3. Yb-doped main fiber amplifier output M^2 measurement at 75.2 W by a Spiricon M2-200 M^2 meter.

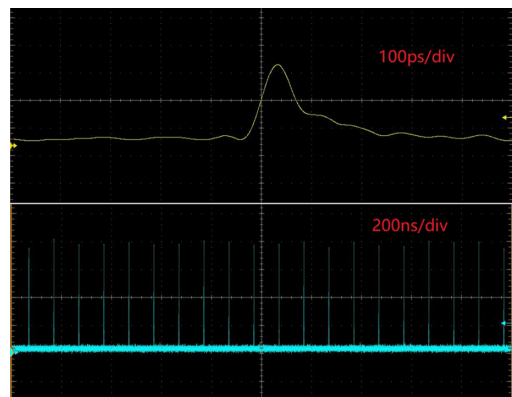


Fig. 4. 1029-nm IR pulse shape and pulse train measured at 75.2-W output power.

measured at different power levels. As can be seen in the figure, the spectral bandwidth gradually becomes broader with the increase of the output power, which may exceed the phase-matching bandwidth of the LBO crystal and cause the decrease in SHG efficiency. The green laser beam profile measured by Ophir NanoScan is shown in Fig. 6(b); it is a clean single mode with a beam ellipticity of better than 95%. The picosecond green laser pulse shape is shown in Fig. 6(a). Compared with the IR laser pulse shape in Fig. 3, it has a much sharper trailing edge

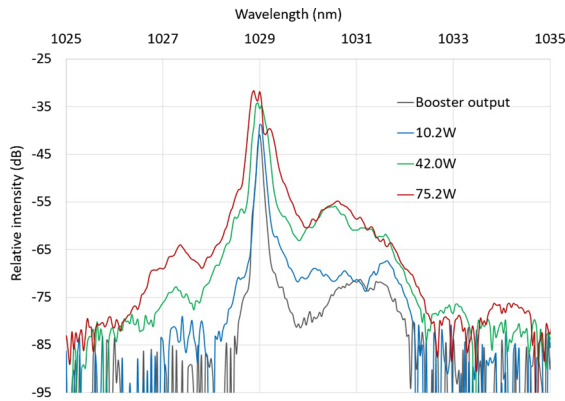


Fig. 5. 1029-nm Yb main fiber amplifier spectrum at different output power levels.

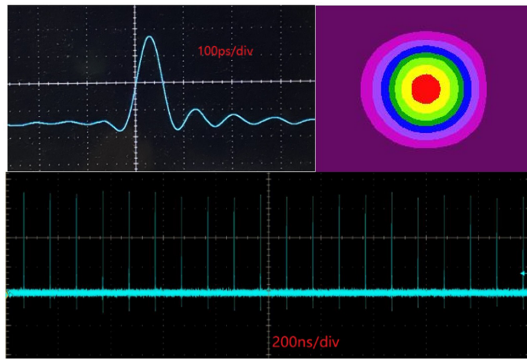


Fig. 6. (top right) Green laser, (top left) pulse shape beam profile, and (bottom) pulse train measured at 43.0-W output.

and the pulse width reduces to 55-ps FWHM. The calculated green laser pulse energy is 4.3 μJ with a peak power of 78.2 kW. The green laser pulse train is shown in Fig. 6(c).

Barium borate (BBO) and CLBO are the two most popular nonlinear crystals for fourth harmonic generation (FHG). Although BBO has a higher optical nonlinear coefficient d_{eff} , the CLBO crystal has lower walk-off, higher acceptance angle, broader spectral bandwidth, and higher damage threshold. In addition, at high input intensity, the BBO crystal is more susceptible to two-photon absorption (TPA) which leads the saturation of the FHG efficiency [13]. Therefore, in this work, a CLBO crystal is selected for FHG. The CLBO has dimensions of 3 mm \times 3 mm \times 20 mm with a type-I critical phase matching cut ($\theta = 65.8^\circ$, $\varphi = 45^\circ$). To increase the damage threshold, both end surfaces are just optically polished without any AR coating. To prevent deliquescence, the CLBO is always stored in a dry and sealed environment when it is not being used in the setup. The crystal was wrapped with indium foil and mounted in an aluminum holder for heat dissipation. A Pellin Broca prism made with UV fused silica glass is used to separate the DUV and the residual green laser beam, as shown in Fig. 1.

It is well known that the efficient nonlinear frequency conversion requires high laser intensity; however, when either the green or DUV laser intensity is high enough, the TPA effects in the nonlinear crystal will be significant and limit the power scaling of the DUV generation. Therefore, to investigate the compromised input intensity for the DUV generation, different green laser focal diameters ($d_0 = 580 \mu\text{m}$, $420 \mu\text{m}$, and $280 \mu\text{m}$)

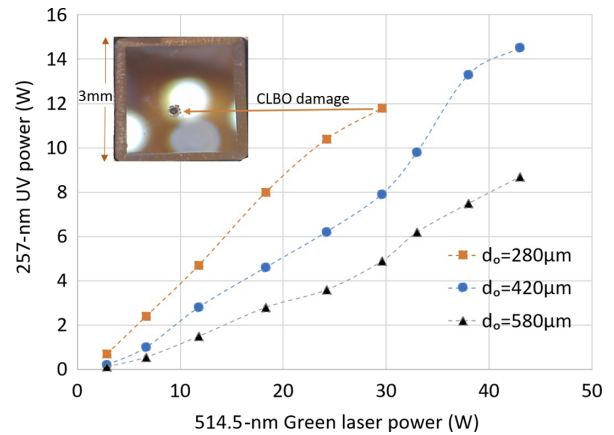


Fig. 7. 257-nm DUV power versus 514-nm green laser power for different focal diameters in CLBO crystal. Inset shows CLBO crystal damage at the output surface.

on the CLBO crystal have been examined. The focal diameters are estimated based on the measured green laser beam size, beam divergence, L3 focal length, and its relative position to the CLBO crystal. Before L3, a half-wave plate with AR coating at 514.5 nm is employed to optimize the polarization of the green laser. At first, a relatively larger focal diameter $d_0 = 580 \mu\text{m}$ has been tested. As shown in in Fig. 7 by the triangle labels, the DUV conversion efficiency increases straightforwardly with the green laser power. At a 43.0-W input power, 8.7 W of 257-nm DUV was generated, corresponding to a FHG efficiency of 20.2%. There is no indication of power saturation and the DUV output is limited by the available green laser power. With a medium focal diameter of $d_0 = 420 \mu\text{m}$, the overall FHG conversion efficiency is higher than that of $d_0 = 580 \mu\text{m}$. At a 38.0-W green laser power, a 13.3-W DUV output was obtained, corresponding to a conversion efficiency of 35.0%. Further increasing the green laser to 43.0 W, the DUV output reaches a maximum of 14.5 W with a FHG conversion efficiency of 33.7%. The slight drop in efficiency might indicate the onset of TPA effects. The highest conversion efficiency was obtained with the tightest focusing $d_0 = 280 \mu\text{m}$. At a green power of 18.3 W, 8.0 W of 257-nm DUV laser was generated, corresponding to a FHG conversion efficiency of 43.7%. Further increasing the green laser power, the TPA becomes more significant and lowers the conversion efficiency. At 29.6-W green laser power, the 257-nm DUV output is 11.8 W, corresponding to an FHG efficiency of 39.9%. Such a tightly focused high-power DUV only lasted for a short time before it caused damage to the CLBO crystal, which is shown by the inset picture in Fig. 7. The damage is located on the output surface of the crystal; therefore, it is the high-intensity DUV rather than the green laser that causes the CLBO damage. The size of the damage spot is estimated to be $\sim 250 \mu\text{m}$, which agrees with the estimated beam size of the focused green laser.

The laser output spectrum is shown in Fig. 8, which is measured by a StellarNet Bluewave compact spectrometer. The spectrometer has been intentionally tilted to receive some residual 514.5-nm green laser so we can see both wavelengths involved in the FHG. The 257-nm DUV laser beam profiles measured at low and medium powers (2.8 W and 9.8 W) with $\omega = 420 \mu\text{m}$ are inserted in Fig. 8. They are single mode laser beams with a certain ellipticity of $\sim 75\%$. The ellipticity is due to the spatial walk-off effects in the nonlinear optics,

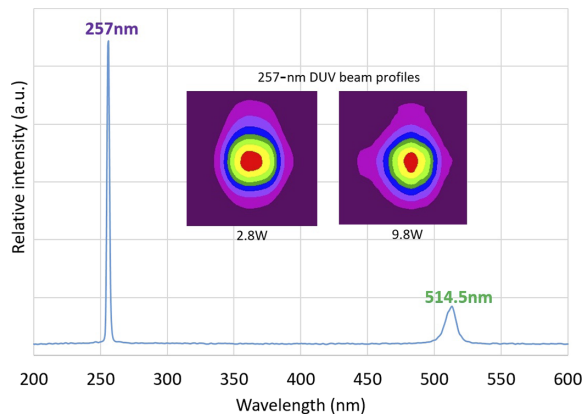


Fig. 8. Laser spectrum measured by StellarNet bluewave compact USB spectrometer. Inset shows 257-nm DUV beam profiles measured by Ophir NanoScan with a focusing condition of $d_0 = 420 \mu\text{m}$.

since the CLBO crystal used here is relatively long (20 mm). Unfortunately, the CLBO crystal was damaged before we could characterize the DUV beam profile at full output power. The 257-nm laser pulse shape is not measured due to the unavailability of a fast photodiode at the DUV wavelength.

With a highly Yb-doped LMA silicate glass fiber as the main amplifier and LBO, CBLO crystals as frequency converters, we demonstrated high-power all-fiberized picosecond green and DUV lasers. With 75.2-W IR at 1029 nm, 43.0 W of green at 514.5 nm and 14.5 W of DUV at 257 nm have been achieved, corresponding to an SHG efficiency of 57.2% and an FHG efficiency of 33.7%, respectively. Different green laser focal diameters on the CLBO crystal have been investigated to optimize the DUV output power and conversion efficiency. It is observed that although tighter focusing results in higher FHG efficiency, it leads to power saturation earlier and may cause nonlinear crystal damage. Such compact, robust, efficient, and powerful picosecond green and DUV lasers may find applications in many fields. The all-fiber-based picosecond green laser

has been commercially available from the company [14] and the development of an industrial DUV laser in progress.

Funding. U.S. Department of Energy (DE-SC0021449).

Acknowledgement. Jihong Geng acknowledges Dr. Sasha Gilevich and her team at SLAC National Accelerator Laboratory for valuable discussion and suggestion on the laser development.

Disclosures. The authors declare no conflicts of interest.

Data availability. Data underlying the results presented in this paper are not publicly available at this time but may be obtained from the authors upon reasonable request.

REFERENCES

1. J. H. Klein-Wiele, J. Bekesi, and P. Simon, *Appl. Phys. A* **79**, 775 (2004).
2. S. P. Banerjee, Z. Chen, and R. Fedosejevs, *Opt. Lasers Eng.* **68**, 1 (2015).
3. Q. Li, T. Ruckstuhl, and S. Seeger, *J. Phys. Chem. B* **108**, 8324 (2004).
4. C. Wagner and N. Harned, *Nat. Photonics* **4**, 24 (2010).
5. S. Gilevich, S. Alverson, S. Carbajo, S. Droste, S. Edstrom, A. Fry, M. Greenberg, R. Lemons, A. Miahnahri, W. Polzin, S. Vetter, and F. Zhou, in *Conference on Lasers and Electro-Optics, OSA Technical Digest* (Optica Publishing Group, 2020), paper SW3E.3.
6. S. Chaitanya Kumar, J. Canals Casals, E. Sanchez Bautista, K. Devi, and M. Ebrahim-Zadeh, *Opt. Lett.* **40**, 2397 (2015).
7. S. Chaitanya Kumar, J. Canals Casals, J. Wei, and M. Ebrahim-Zadeh, *Opt. Express* **23**, 28091 (2015).
8. M. Müller, A. Klenke, T. Gottschall, R. Klas, C. Rothhardt, S. Demmler, J. Rothhardt, J. Limpert, and A. Tünne rmann, *Opt. Lett.* **42**, 2826 (2017).
9. J. He, D. Lin, L. Xu, M. Beresna, M. Zervas, S. Alam, and G. Brambilla, *Opt. Express* **26**, 6554 (2018).
10. Q. Fu, N. Hanrahan, L. Xu, S. Lane, D. Lin, Y. Jung, S. Mahajan, and D. Richardson, *Opt. Express* **29**, 42485 (2021).
11. S. Jiang, T. Luo, Q. Wang, and L. Pan, "Rare-earth doped gain fibers," U.S. Patent 9581760 (28 February 2017).
12. S. Jiang, T. Luo, Q. Wang, and L. Pan "Ultrashort pulse fiber amplifier using rare-earth doped gain fibers," U.S. Patent 9722390 (1 August 2017).
13. O. Novák, H. Turčičová, M. Smrž, T. Miura, A. Endo, and T. Mocek, *Opt. Lett.* **41**, 5210 (2016).
14. Advalue Photonics Inc. EVERESTpico Green Picosecond Laser <https://advaluephotonics.com/products/everestpico-green-picosecond-laser-ap-515p>